

Data-Driven Robust Control Using Prediction Error Bounds Based on Perturbation Analysis

Baiwei Guo, Yuning Jiang, Colin N. Jones, Giancarlo Ferrari-Trecate

Abstract

For linear systems, many data-driven control methods rely on the behavioral framework, using historical data of the system to predict the future trajectories. However, measurement noise introduces errors in predictions. When the noise is bounded, we propose a method for designing historical experiments that enable the computation of an upper bound on the prediction error. This approach allows us to formulate a minmax control problem where robust constraint satisfaction is enforced. We derive an upper bound on the suboptimality gap of the resulting control input sequence compared to optimal control utilizing accurate measurements. As demonstrated in numerical experiments, the solution derived by our method can achieve constraint satisfaction and a small suboptimality gap despite the measurement noise.

I. INTRODUCTION

With advancements in sensing, storage, and computation technologies, the availability of data has significantly increased. This enables the design of controllers that are both safe (i.e., satisfying constraints) and near-optimal in the presence of uncertainties [1], [2].

Control synthesis methods can be broadly categorized as either *model-based* or *model-free*. Model-based methods involve two stages: collecting historical system trajectories to identify a parametric model for system dynamics, and utilizing this model to calculate optimal control decisions. Classical methods like LQG control [3] and feedback linearization [4] fall under this category. A common drawback is that the involved system identification tasks can be demanding especially when the model structure is unknown, requiring time-consuming procedures such as data preprocessing, model selection, and validation [5].

This work has been supported by the Swiss National Science Foundation under the NCCR Automation (grant agreement 51NF40_80545).

Baiwei Guo and Giancarlo Ferrari-Trecate are with the DECODE group, Institute of Mechanical Engineering, EPFL, Switzerland. email:{baiwei.guo, giancarlo.ferraritrecate@epfl.ch}

Yuning Jiang and Colin N. Jones are with the PREDICT group, Institute of Mechanical Engineering, EPFL, Switzerland. email:{yuning.jiang, colin.jones@epfl.ch}

Additionally, regarding the accuracy of the derived model under measurement noise, existing upper bounds for identification errors rely on the unknown ground-truth system model instead of empirical data [6], [7]. Therefore, without further assumptions, these bounds cannot be directly used in robust control.

In contrast, model-free methods derive the optimal control inputs directly from data without explicitly identifying the system model, simplifying the formulation process. For example, the authors of [8] use a maximum likelihood framework to obtain an optimal data-driven model for trajectory prediction. This way, one can avoid separate ML-based model identification and Kalman Filter for state estimation. Model-free methods are also highly effective in robust constraint satisfaction [9] and optimal control of some nonlinear dynamics [10]. However, a complete theoretical explanation of these advantages are still lacking.

Many model-free methods are based on Willems' fundamental lemma [11] for linear systems. This lemma states that, under the assumption of persistent excitation, any trajectory of a given linear system is a linear combination of a Hankel matrix's columns where the Hankel matrix consists of the historical trajectories. It allows us to represent the system directly with the data instead of identifying a parametric model. The system representation based on the Hankel matrix is called a behavioral model.

In this paper, we develop a behavioral-model-based approach toward robust control of linear systems. Specifically, we aim to minimize the worst-case regulation cost and satisfy constraints under bounded output measurement noise. Several existing works approximately solve this problem from different perspectives and under different assumptions. For input-output systems whose states are not directly measurable, [12] optimizes an output feedback controller by using the behavioral model to identify the system's impulse response. The derived controller results in a higher cost than the optimal one due to the measurement noise and the authors derive a bound for the suboptimality gap. The drawback of this method is that both the suboptimality bound and the satisfaction of the constraints rely on a bootstrap procedure which requires extra resampling and computation. Moreover, a rigorous analysis on the accuracy of bootstrap results using finite samples is still lacking [13]. In contrast, without the efforts of identification, [14] minimizes the worst-case trajectory tracking cost by reformulating the minmax problem into a Semidefinite Program through the S-lemma. However, the optimality results in [14] rely on the assumption that the noise sequence satisfies a cumulative quadratic constraint. Therefore, they do not hold when all entries of the noise sequence are known to satisfy box constraints. To address this issue, [15] adopts a different reformulation where model misfit penalty is added to the tracking cost. The involved minmax problem is solvable by robust optimization techniques and the authors derive a suboptimality gap bound. However, this bound is conservative in the sense that it does not vanish when the noise decreases to zero.

To develop a method that enjoys both a less conservative suboptimality gap and the guarantee of constraint satisfaction, we leverage perturbation analysis for assessing the influence of measurement noise on the behavioral-model predictions. Research on perturbation analysis of data-driven prediction includes [16], [17] and [18]. In [16], the authors use a cost function similar with the one in [15], aiming to minimize the sum of the misfit penalty and the tracking cost. Therefore, the prediction error upper bound relies on a variable related to the optimal control task and thus can only be evaluated after the optimal control problem has been solved. In contrast, the robust fundamental lemma proposed in [17] gives a prediction error analysis independent of control tasks, but it is limited to input-state systems and one-step-ahead prediction. The work in [18] extends [17] by deriving lower bounds for the singular values of the Hankel matrix in the behavioral model for input-output systems. However, the lower bounds depend on the unknown ground truth system model.

In this paper, we aim to upperbound the error of behavioral-model-based prediction for general input-output linear systems and utilize this bound for minmax robust control with guarantees of constraint satisfaction. Our main contributions are the following:

- We propose an input generation strategy to collect historical data under bounded measurement noise for the construction of a Page matrix (a variant of Hankel matrix, see [19]) enabling the derivation of an error bound of the data-driven predictions, which only relies on the noisy data. This bound is valid when the historical inputs achieve sufficient “persistent-excitation-to-noise ratio” (rigorously stated in Assumption 8) and the observability index (see Definition 4) is identified correctly. The first condition can be satisfied if collecting multiple historical data sets for averaging the noisy measurements or enlarging the input signals is allowed. We achieve the second through a data-driven method with correctness guarantee.
- For unconstrained regulation of MISO systems, in order to minimize the worst-case cost, we utilize the new prediction error bound to formulate a minmax problem and bound the suboptimality gap. The derived bound decreases to zero as the measurement noise converges to zero. This scheme can be extended to regulation of MIMO systems and robust constraint satisfaction.

The rest of this paper is organized as follows: in Section II, we introduce the basics of data-driven control and formulate the robust control problem. Section III focuses on MISO systems with no input output constraints and addresses perturbation analysis on the noisy behavioral model used for trajectory prediction. The robust control scheme is proposed in Section IV where the associated upper bound of the worst-case cost derived by using perturbation analysis is minimized and the suboptimality gap is bounded. We extend our method for regulation of MIMO systems and for robust constraint satisfaction

in Section V. Experiments illustrating the performance of the proposed approach are shown in Section VI.

Notations: Given a time-varying vector variable v , we use v_t to denote its value at time instant t , let $[t_1, t_2] = \{t_1, t_1+1, \dots, t_2\}$ and set $v_{[t_1, t_2]} := \{v_{t_1}, v_{t_1+1}, \dots, v_{t_2}\}$, $\text{col}(v_{[t_1, t_2]}) := \begin{bmatrix} v_{t_1}^\top & v_{t_1+1}^\top & \dots & v_{t_2}^\top \end{bmatrix}^\top$. We use $\|x\|_i$ to denote the ℓ_i norm of x . Moreover, $\|x\|$ is the ℓ_2 norm. Given positive semidefinite matrix Q , the term $\|x\|_Q^2$ denotes $x^\top Q x$. For a matrix M , $\|M\|_i$ denotes the matrix i -norm while $\|M\|_{\max} := \max_{i,j} |m_{ij}|$ and $\|M\| := \|M\|_2$. We also denote $\sigma_{\min}(M)$ as the smallest singular value of M and $\sigma_{\max}(M)$ as the largest. We use $M_{i,\cdot}$ to denote the i -th row, $M_{\cdot,i}$ the i -th column and $M_{i:j,\cdot}$ the submatrix consisting of the rows of M from the i -th to the j -th. For a given $x \in \mathbb{R}$, we use notation $\lfloor x \rfloor$ to denote the floor function, i.e., $\lfloor x \rfloor = \max\{z \in \mathbb{Z} \mid z \leq x\}$. For $y \in \mathbb{R}^n$ and $r > 0$, we let $\mathcal{B}(y, r) := \{x : \|x - y\| \leq r\}$. The identity matrix with n rows is denoted as I_n . The pseudo-inverse of a matrix H is written as H^\dagger .

II. PRELIMINARIES AND PROBLEM FORMULATION

A. Preliminaries: data-driven description of linear systems

This paper considers the regulation of a discrete-time linear time-invariant (LTI) system with the following controllable and observable minimal realization,

$$x_{t+1} = Ax_t + Bu_t, \quad y_t = Cx_t + Du_t, \quad (*)$$

where $u_t \in \mathbb{R}^m$, $y_t \in \mathbb{R}^p$ and $x_t \in \mathbb{R}^{n_x}$. We assume that n_x and the system matrices A, B, C, D are unknown. Instead of identifying the system matrices, we utilize a behavioral model to characterize the possible trajectories in a horizon of length L . To build this system representation, we excite the linear system with an input sequence $u_{[1, T]}$ and collect the output data $y_{[1, T]}$, where $T > L$. The L -Page matrix of $u_{[1, T]}$ is given by

$$\mathcal{P}_L(u_{[1, T]}) := \begin{bmatrix} u_1 & u_{L+1} & \dots & u_{l_h L - L + 1} \\ u_2 & u_{L+2} & \dots & u_{l_h L - L + 2} \\ \vdots & \vdots & \ddots & \vdots \\ u_L & u_{2L} & \dots & u_{l_h L} \end{bmatrix}$$

where $l_h = \lfloor \frac{T}{L} \rfloor$ denotes the number of columns [19]. To evaluate whether the input sequence $u_{[1, T]}$ along with the resulting outputs is sufficiently informative to uniquely determine system $(*)$, we introduce the following definition analogous to persistent excitation in system identification.

Definition 1 ([19]). For $L, T, d \in \mathbb{Z}^+$, we say the input sequence $u_{[1,T]}$ is L -Page exciting of order d if the following matrix has full row rank,

$$\mathcal{P}_{L,d}(u_{[1,T]}) := \begin{pmatrix} \mathcal{P}_L(u_{[1,T-(d-1)L]}) \\ \mathcal{P}_L(u_{[L+1,T-(d-2)L]}) \\ \vdots \\ \mathcal{P}_L(u_{[L(d-1)+1,T]}) \end{pmatrix}.$$

By using the collected input output data $(u_{[1,T]}, y_{[1,T]})$, called *historical*, one might be able to determine whether another trajectory $(u_{[1,L]}^r, y_{[1,L]}^r)$, called *recent*, is generated by system (*). Rigorously, we have the following result, which is a variant of the well-known Willem's Fundamental Lemma [11].

Lemma 2 ([19, Theorem 2.1]). For the LTI system described in (*), given a T -length historical trajectory $(u_{[1,T]}, y_{[1,T]})$ where $u_{[1,T]}$ is L -Page exciting of order $n_x + 1$ and the L -length recent trajectory $(u_{[1,L]}^r, y_{[1,L]}^r)$, there exists $x_{[1,L]}^r$ with $x_i \in \mathbb{R}^{n_x}$, $1 \leq i \leq L$, such that $(x_{[1,L]}^r, u_{[1,L]}^r, y_{[1,L]}^r)$ satisfies (*) if and only if there exists a vector $g \in \mathbb{R}^{l_h}$ such that

$$\begin{bmatrix} \mathcal{P}_L(u_{[1,T]}) \\ \mathcal{P}_L(y_{[1,T]}) \end{bmatrix} g = \begin{bmatrix} \text{col}(u_{[1,L]}^r) \\ \text{col}(y_{[1,L]}^r) \end{bmatrix}. \quad (1)$$

B. Problem formulation: robust control under measurement noise

Given the historical data $(u_{[1,T]}, y_{[1,T]})$ where $u_{[1,T]}$ is L -Page exciting of order $n_x + 1$ and an l_p -long initial trajectory $(u_{[1,l_p]}^r, y_{[1,l_p]}^r)$ with $l_p < L$, we consider the following regulation problem for the trajectory $(u_{[1,T]}^r, y_{[1,T]}^r)$ from $t = l_p + 1$ to $t = L$:

$$\begin{aligned} \min_{u_{[l_p+1,L]}^r, y_{[l_p+1,L]}^r} & \sum_{i=1}^{L-l_p} (||u_{l_p+i}^r||^2 + ||y_{l_p+i}^r||^2) \\ \text{s.t.} & \text{ there exists } g \text{ such that} \end{aligned} \quad (2)$$

$$u_{[1,T]}, y_{[1,T]}, u_{[1,L]}^r, y_{[1,L]}^r \text{ satisfy (1).}$$

For convenience, we let $l_f = L - l_p$ and use the following notations for historical data,

$$\begin{aligned} U_p &= \begin{bmatrix} I_{ml_p} & 0 \end{bmatrix} \mathcal{P}_L(u_{[1,T]}), U_f = \begin{bmatrix} 0 & I_{ml_f} \end{bmatrix} \mathcal{P}_L(u_{[1,T]}), \\ Y_p &= \begin{bmatrix} I_{pl_p} & 0 \end{bmatrix} \mathcal{P}_L(y_{[1,T]}), Y_f = \begin{bmatrix} 0 & I_{pl_f} \end{bmatrix} \mathcal{P}_L(y_{[1,T]}) \end{aligned} \quad (3)$$

and for recent data,

$$\begin{aligned} u_p &= \text{col}(u_{[1,l_p]}^r), u_f = \text{col}(u_{[l_p+1,L]}^r), \\ y_p &= \text{col}(y_{[1,l_p]}^r), y_f = \text{col}(y_{[l_p+1,L]}^r). \end{aligned} \quad (4)$$

In practice, output measurements are subject to noise. Specifically, for any $i \in [1, \dots, T]$, $j \in [1, \dots, l_p]$, there exist noise vectors $w_i, w_j^r \in \mathbb{R}^p$ such that the measurements are $\hat{y}_i = y_i + w_i$ and $\hat{y}_j^r = y_j^r + w_j^r$. We build \hat{Y}_p, \hat{Y}_f and \hat{y}_p from $\hat{y}_{[1,T]}$ and $\hat{y}_{[1,l_p]}^r$ as noisy counterparts of Y_p, Y_f and y_p . In this paper, we only consider bounded noise, as stated in the following assumption.

Assumption 3. For the noisy measurements $\hat{Y}_p, \hat{Y}_f, \hat{y}_p$, corresponding to Y_p, Y_f, y_p , the following holds,

$$\max\{\|\hat{Y}_p - Y_p\|_{\max}, \|\hat{Y}_f - Y_f\|_{\max}, \|\hat{y}_p - y_p\|_{\infty}\} \leq \delta,$$

where $\delta > 0$ is a known constant.

Given a fixed control strategy, different noise realizations lead to different performances. To attenuate the influence of the uncertainties, we aim to **design a robust control scheme where the worst-case regulation cost is minimized**. In general, the worst-case cost is hard to compute and we will provide an upper bound $c_{\text{worst}}(u_f)$ to it given the historical data $u_{[1,T]}$, $\hat{y}_{[1,T]}$ and the recent data u_p and \hat{y}_p . We formulate the robust control problem as

$$u_f^* = \operatorname{argmin}_{u_f} c_{\text{worst}}(u_f).$$

This way, we ensure that the true cost induced by u_f^* is less than $c_{\text{worst}}(u_f^*)$.

In Section IV we propose a formulation of $c_{\text{worst}}(u_f)$. But before that, in Section III, by assuming u_f is given, we introduce tools of data-driven prediction based on behavioral models and conduct perturbation analysis, which allows us to estimate the worst-case cost by using the noisy data. To avoid bulky statements, we only consider the MISO case in Sections III and IV, while the extension to the MIMO case is presented in Section V.

III. DATA-DRIVEN PREDICTION WITH PERTURBATION ANALYSIS FOR MISO SYSTEMS

In this section, we investigate, for MISO systems, a data-driven prediction method that generates an estimate \hat{y}_f for y_f based on historical data along with u_p, \hat{y}_p and u_f . Specifically, we propose a method for generating historical data enabling the derivation of an upper bound for the prediction error. This ingredient is essential for the computation of upper bounds to worst-case costs in Section IV.

A. The proposed data-driven prediction scheme

For MISO systems, we adopt the data-driven prediction method used in the framework of **PEM-MPC**¹ proposed in [20]. Specifically, we look into the following prediction scheme

$$\hat{g}(u_f) = \hat{H}^T \hat{b}(u_f), \quad \hat{y}_f(u_f) = \hat{Y}_f \hat{g}(u_f), \quad \text{where } \hat{H} = \begin{bmatrix} U_p^T & \hat{Y}_p^T & U_f^T \end{bmatrix}^T, \quad \hat{b}(u_f) = \begin{bmatrix} u_p^T & \hat{y}_p^T & u_f^T \end{bmatrix}^T. \quad (5)$$

¹PEM stands for *Prediction Error Method*.

We also define the noiseless counterparts of $\hat{H}, \hat{b}(u_f), \hat{g}(u_f), \hat{y}_f(u_f)$ in (5) as $\bar{H}, \bar{b}(u_f), \bar{g}(u_f), \bar{y}_f(u_f)$. One can easily verify that $\|\bar{g}(u_f)\| = \min\{\|g\| : \bar{H}g = \bar{b}(u_f) \text{ and } Y_f g = \bar{y}_f(u_f)\}$. Before elaborating on the historical data collected and the construction of \hat{H} in Assumption 5, we introduce the concept of observability index.

Definition 4. We say l_o is the observability index of the system (*) if the l_o is the smallest positive integer l such that the observability matrix $\mathcal{O}(l) := \begin{bmatrix} C^\top & (CA)^\top & \cdots & (CA^{l-1})^\top \end{bmatrix}^\top$ is full column rank.

Assumption 5. Given horizon length $L > l_o$, the historical inputs of the MISO system (*) are generated using the following setting:

$$x_1 = 0, \quad (6a)$$

$$u_{[1,L]}, u_{[L+1,2L]}, \dots, u_{[4L^2+1,4L^2+L]} \stackrel{\text{i.i.d.}}{\sim} \mathcal{Q}, \quad (6b)$$

$$T \geq 4L^2 + L \text{ and } u_{[1,T]} \text{ is } L\text{-Page exciting of order } n_x + 1, \quad (6c)$$

where \mathcal{Q} is a probability distribution such that for $x \in \mathbb{R}^{mL}$

$$\text{if } x \sim \mathcal{Q} \text{ then for any subspace } V \subsetneq \mathbb{R}^{mL}, \mathbb{P}(\{x \in V\}) = 0. \quad (7)$$

The Page matrices $U = \mathcal{P}_L(u_{[1,T]})$ and $\hat{Y} = \mathcal{P}_L(\hat{y}_{[1,T]})$ are split into $U_p, U_f, \hat{Y}_p, \hat{Y}_f$ using (3) with

$$l_p = l_o, \quad (8)$$

and \hat{H} is built using (5).

For identification of l_o using data, we refer to Section III-C and Algorithm 1. Under Assumption 5, we will see in Section III-B that the noiseless matrix \bar{H} is almost surely full row rank. This property is essential for upperbounding the prediction error resulting from (5). The reason is that, if \bar{H} has a zero singular value, even infinitesimal measurement noise can result in a huge prediction error due to the use of the pseudoinverse in (5).

B. Perturbation analysis

We show in Theorem 6 and Theorem 10 that the prediction error resulting from the scheme (5) can be bounded.

Theorem 6. Under Assumption 5, we have $\mathbb{P}(\{\bar{H} \text{ is full row rank}\}) = 1$.

The proof of Theorem 6 is given in Appendix B.

Remark 7. *Theorem 6 does not hold for MIMO systems. As a simple example, when there are two outputs measuring the same quantity, almost surely the noiseless \bar{H} is not full row rank.*

By utilizing Theorem 6, we show in Theorem 10 that, when the measurement noise is sufficiently small (as indicated below), the prediction errors given by the least-square solution (5) can be bounded.

Assumption 8. *With \hat{H} constructed according to Assumption 5, we have*

$$\delta < \frac{\sigma_{\min}(\hat{H})}{2l_h}. \quad (9)$$

Remark 9. *As will be shown later in Theorem 10, under Assumption 8, an upper bound for the prediction error is roughly proportional to $\sigma_{\min}(\hat{H})^{-1}$. Therefore, we can regard $\sigma_{\min}(\hat{H})$ as a measure of “persistent excitation” and thus (9) requires the “persistent-excitation-to-noise ratio” to be sufficiently large. In [16, Lemma 1], a similar assumption is made. To satisfy Assumption 8, one can decrease the noise magnitude by collecting multiple historical data sets and using averaging techniques if the entries of the noise sequence are independent and identically distributed (for details see Remark 17). Since from [21, Theorem 4.3] we have*

$$\sigma_{\min}(\hat{H}) \geq \sigma_{\min}(\bar{H}) - \|\hat{H} - \bar{H}\|, \quad (10)$$

we can also amplify the historical input signals in (6) for obtaining a larger $\sigma_{\min}(\bar{H})$ and hence increasing $\sigma_{\min}(\hat{H})$.

Theorem 10. *We denote $\bar{\Delta}_g(u_f) := \bar{g}(u_f) - \hat{g}(u_f)$ and $\bar{\Delta}_{y_f}(u_f) := \bar{y}_f(u_f) - \hat{y}_f(u_f)$. If Assumption 8 holds, we have for MISO systems*

$$\|\bar{\Delta}_g(u_f)\| \leq \mathcal{C}(u_f)\delta, \text{ where } \mathcal{C}(u_f) = 2\sigma_{\min}(\hat{H})^{-1}(\sqrt{l_p} + l_h\|\hat{g}(u_f)\|), \text{ and}$$

$$\|\bar{\Delta}_{y_f}(u_f)\| \leq \mathcal{C}(u_f)\|\hat{Y}_f\|\delta + l_h(\|\hat{g}(u_f)\| + \mathcal{C}(u_f))\delta.$$

Proof. We let $E := \hat{H} - \bar{H}$. Due to Assumption 3, we have

$$\|E\| \leq l_h\delta. \quad (11)$$

Then the following inequalities hold,

$$\begin{aligned}
\frac{\sigma_{\min}(\widehat{H})}{2} \|\hat{g}(u_f) - \bar{g}(u_f)\| &\leq (\sigma_{\min}(\widehat{H}) - \|E\|) \|\hat{g}(u_f) - \bar{g}(u_f)\| \\
&\leq \sigma_{\min}(\widehat{H} - E) \|\hat{g}(u_f) - \bar{g}(u_f)\| \\
&\leq \|\overline{H}(\hat{g}(u_f) - \bar{g}(u_f))\| \\
&\leq \|\widehat{H}\hat{g}(u_f) - \overline{H}\bar{g}(u_f) + (\overline{H} - \widehat{H})\hat{g}(u_f)\| \\
&\leq \|\hat{b}(u_f) - \bar{b}(u_f)\| + \|E\| \cdot \|\hat{g}(u_f)\| \\
&= (\sqrt{l_p} + l_h \|\hat{g}(u_f)\|) \delta,
\end{aligned} \tag{12}$$

where the first inequality is due to (9) in Assumption 8, the second results from (10) and $\hat{b}(u_f)$ is defined in (5). By simplifying (12), we have

$$\|\overline{\Delta}_g(u_f)\| \leq \mathcal{C}(u_f) \delta.$$

Based on this inequality, we have

$$\begin{aligned}
\|\hat{y}_f(u_f) - \bar{y}_f(u_f)\| &= \|\widehat{Y}_f(\hat{g}(u_f) - \bar{g}(u_f)) + (\widehat{Y}_f - Y_f)\bar{g}(u_f)\| \\
&\leq \|\widehat{Y}_f\| \cdot \|\hat{g}(u_f) - \bar{g}(u_f)\| + \|\widehat{Y}_f - Y_f\| \cdot \|\bar{g}(u_f)\| \\
&\leq \|\widehat{Y}_f\| \cdot \|\hat{g}(u_f) - \bar{g}(u_f)\| + \\
&\quad l_h \delta (\|\hat{g}(u_f)\| + \|\bar{g}(u_f) - \hat{g}(u_f)\|) \\
&\leq \mathcal{C}(u_f) \|\widehat{Y}_f\| \delta + l_h (\|\hat{g}(u_f)\| + \mathcal{C}(u_f)) \delta.
\end{aligned} \tag{13}$$

□

In the literature, similar results on perturbation analysis accounting for measurement noise can be found in [7] and [6]. However, the associated bounds utilize the unknown true system model. In the behavioral model framework, [16] also derives a prediction error bound after solving an optimal control problem. Therefore, the bound is only valid for the optimal control sequence u_f^* determined by the specific problem formulation. In contrast, our upper bound in Theorem 10 can be calculated directly from the noisy data for any given u_f . This feature allows us to formulate in Sections IV and V a min-max regulation problem where robust constraint satisfaction can be enforced.

C. Data-driven identification of l_o

We discuss the identification of l_o , which is needed in the construction of \widehat{H} for satisfying Assumption 5. For this aim, we discuss in Proposition 11 whether \overline{H} almost surely has full rank when Assumption 5 does not hold. Based on this result, we propose a method to identify l_o .

Proposition 11. *If Assumption 5 does not hold because $l_p < l_o$, then*

$$\mathbb{P}(\{\overline{H} \text{ is full row rank}\}) = 1.$$

Furthermore, if $l_p > l_o$, $\mathbb{P}(\{\overline{H} \text{ is full row rank}\}) = 0$.

The proof is reported in Appendix C. Theorem 6 and Proposition 11 say that l_o is the largest value for l_p such that the constructed \overline{H} is full row rank. We notice that the noise matrix $E = \hat{H} - \overline{H}$ satisfies that $\|E\| \leq l_h \delta$ ². Therefore, if \overline{H} is not full row rank, i.e., $\sigma_{\min}(\overline{H}) = 0$, we have

$$\sigma_{\min}(\hat{H}) \leq \sigma_{\min}(\overline{H}) + \sigma_{\max}(E) \leq l_h \delta. \quad (14)$$

By utilizing (14), we propose Algorithm 1 for identification of l_o and show the correctness of the derived result in Proposition 12.

Proposition 12. *Under Assumption 8, if $L > l_o$, Algorithm 1 returns l_o , the true observability index, almost surely.*

Proof. From Assumption 8 and (14), we know that $\sigma_{\min}(\hat{H}) \geq 2l_h \delta$ if $l_p = l_o$ and $\sigma_{\min}(\hat{H}) \leq l_h \delta$ if $l_p > l_o$. Since Algorithm 1 terminates when $\sigma_{\min}(\hat{H}) \leq l_h \delta$ is verified, we only need to show that $\sigma_{\min}(\hat{H}) > l_h \delta$ almost surely if $l_p < l_o$.

In the remainder of this proof, we denote with $[U_{p,k}^\top \ U_{f,k}^\top]^\top$ and $[\hat{Y}_{p,k}^\top \ \hat{Y}_{f,k}^\top]^\top$ the partitions of the Page matrices U and Y , respectively, where $U_{p,k}$ has km rows and $Y_{p,k}$ has kp rows. Correspondingly, we write $\hat{H}_k := [U_{p,k}^\top \ \hat{Y}_{p,k}^\top \ U_{f,k}^\top]^\top$. We notice that \hat{H}_k is a submatrix consisting of a fraction of \hat{H}_{l_o} 's rows and \hat{H}_{l_o} is full row rank almost surely (Theorem 6). According to Lemma 20 in Appendix D, we have that almost surely $\sigma_{\min}(\hat{H}_k) \geq \sigma_{\min}(\hat{H}_{l_o}) \geq 2l_h \delta$ for any $k < l_o$. \square

Remark 13. *We have another heuristic method which can be used as supplement to Algorithm 1 for the case when Assumption 8 is not satisfied. Specifically, in Line 1 of Algorithm 1, after deriving $(u_{[1,T]}, \hat{y}_{[1,T]})$, we can generate several extra historical trajectories $(u(\alpha)_{[1,T]}, y(\alpha)_{[1,T]})$ using the initial state $x_1 = 0$ and the input sequence $u(\alpha)_{[1,T]} = \alpha u_{[1,T]}$ for different values of α . Based on the data, we can construct Page matrices $U(\alpha), Y(\alpha)$. In Lines 4 and 5, we obtain the submatrices $U_p(\alpha), U_f(\alpha), \hat{Y}_p(\alpha), \hat{Y}_f(\alpha)$ and $\hat{H}(\alpha)$. Due to the linearity of the system and the zero initial state, we have $\overline{H}(\alpha) = \alpha \overline{H}(1)$ and thus $\sigma_{\min}(\overline{H}(\alpha))$ is proportional to α if $\sigma_{\min}(\overline{H}(1)) \neq 0$. Therefore, when observing that $\sigma_{\min}(\hat{H}(1))$ increases approximately proportionally with α , we claim that $\sigma_{\min}(\overline{H}(1)) \neq 0$.*

²To show this result, one only needs Cauchy–Schwarz inequality and Assumption 3.

Algorithm 1 Data-driven observability index identification for MISO systems

Input: horizon length L for the Page matrices

Output: the system order l_o

- 1: Use (6) to generate historical data $(u_{[1,T]}, \hat{y}_{[1,T]})$ to construct Page matrices $U = \mathcal{P}_L(u_{[1,T]})$ and $\hat{Y} = \mathcal{P}_L(\hat{y}_{[1,T]})$.
 - 2: $k \leftarrow 1, \text{TER} = 0$
 - 3: **while** $\text{TER} = 0$ **do**
 - 4: Partition $U = [U_p^\top \ U_f^\top]^\top$, $\hat{Y} = [\hat{Y}_p^\top \ \hat{Y}_f^\top]^\top$ such that U_p has km rows (i.e., $l_p = k$)
 - 5: Build $\hat{H} = [U_p^\top \ \hat{Y}_p^\top \ U_f^\top]^\top$
 - 6: **if** $\sigma_{\min}(\hat{H}) \leq l_h \delta$ **then**
 - 7: $l_o \leftarrow k - 1, \text{TER} \leftarrow 1$
 - 8: **end if**
 - 9: $k \leftarrow k + 1$
 - 10: **end while**
-

IV. ROBUST CONTROL FOR REGULATION OF MISO SYSTEMS WITH SUBOPTIMALITY GUARANTEE

In this section, we propose a data-driven robust control method for MISO systems, where we use the prediction error bounds in Theorem 10 to calculate $c_{\text{worst}}(u_f)$, an upperbound to the regulation cost. To justify that this upperbound is not too conservative, we study the suboptimality of the derived input sequence and compare it with the optimal input sequence. The extension to multiple-output systems is provided in Section V.

With the notation $\Delta := \{\Delta_{Y_p}, \Delta_{Y_f}, \Delta_{y_p}\}$, the robust regulation problem is formulated as the following bilevel program where the inner problem calculates an upperbound for the worst-case cost and the outer problem optimizes the input such that the cost upperbound is minimized,

$$\min_{u_f} \max_{\Delta, g, y_f} y_f^\top y_f + u_f^\top u_f \quad (15a)$$

$$\text{s.t.} \quad \begin{bmatrix} U_p \\ \hat{Y}_p \\ U_f \\ \hat{Y}_f \end{bmatrix} g + \begin{bmatrix} 0 \\ \Delta_{Y_p} \\ 0 \\ \Delta_{Y_f} \end{bmatrix} g = \begin{bmatrix} u_p \\ \hat{y}_p \\ u_f \\ y_f \end{bmatrix} + \begin{bmatrix} 0 \\ \Delta_{y_p} \\ 0 \\ 0 \end{bmatrix} \quad (15b)$$

$$\max \left(\|\Delta_{Y_p}\|_{\max}, \|\Delta_{Y_f}\|_{\max}, \|\Delta_{y_p}\|_{\infty} \right) \leq \delta \quad (15c)$$

$$\|g - \hat{g}(u_f)\|^2 \leq \mathcal{C}^2(u_f) \delta^2. \quad (15d)$$

where $\mathcal{C}(u_f)$ is defined in Theorem 10. We use the alternating optimization method in [22] to solve problem (15) (for details see Section VI-A). We denote the solution to the outer problem as \tilde{u}_f . Given any input sequence u_f , we let $\bar{c}(u_f)$ be the resulting true regulation cost and $c_{\text{worst}}(u_f)$ be the optimal objective value of the inner problem of (15). In the following theorem, we show that $c_{\text{worst}}(u_f)$ is indeed an upperbound to the true regulation cost.

Theorem 14. *If Assumptions 3, 5 and 8 hold, for any u_f we have $c_{\text{worst}}(u_f) \geq \bar{c}(u_f)$.*

Proof. The noise realization $(\bar{\Delta}_{Y_p}, \bar{\Delta}_{Y_f}, \bar{\Delta}_{y_p})$ satisfies that

$$\max(\|\bar{\Delta}_{Y_p}\|_{\max}, \|\bar{\Delta}_{Y_f}\|_{\max}, \|\bar{\Delta}_{y_p}\|_{\infty}) \leq \delta.$$

With the vector $\bar{g}(u_f)$ we can reconstruct the noiseless system output, i.e., $(\hat{Y}_p + \bar{\Delta}_{y_p})\bar{g}(u_f) = y_p$, $(\hat{Y}_f + \bar{\Delta}_{y_f})\bar{g}(u_f) = \bar{y}_f(u_f)$. Now we see that $u_f, \bar{\Delta}_{Y_p}, \bar{\Delta}_{Y_f}, \bar{\Delta}_{y_p}, \bar{g}(u_f)$, and $\bar{y}_f(u_f)$ satisfy (15b), (15c) and the corresponding regulation cost is $\bar{c}(u_f)$. Meanwhile, considering the error bounds in Theorem 10, the constraint (15d) is also satisfied. Since $c_{\text{worst}}(u_f)$ is the maximum cost in the inner problem of (15), we have $c_{\text{worst}}(u_f) \geq \bar{c}(u_f)$. \square

In (15), the outer problem seeks a u_f that minimizes this upperbound. Similar ideas that minimize a cost upperbound can be found in [6], [12]. To discuss the conservativeness of this approach, we need to bound the suboptimality of the solution to (15) when compared to the noiseless case. To this aim, we define the tuple $\hat{\mathcal{Y}} := (\hat{Y}_p, \hat{Y}_f, \hat{y}_p)$, consider the control input sequences

$$\begin{aligned} \hat{u}_f^* &:= \operatorname{argmin}_{u_f} \|\hat{y}_f(u_f)\|^2 + \|u_f\|^2, \\ u_f^* &:= \operatorname{argmin}_{u_f} \|\bar{y}_f(u_f)\|^2 + \|u_f\|^2, \end{aligned} \tag{16}$$

and bound the error $\|\hat{u}_f^* - u_f^*\|$ in the following lemma whose proof is given in Appendix E.

Lemma 15. *Under Assumption 3, 5 and 8, we define the following polynomials in δ ,*

$$\begin{aligned} \mathcal{F}_1(\delta, \hat{\mathcal{Y}}) &:= 2l_h \|\hat{H}^\dagger\| (1 + 4\|\hat{Y}_p\| \cdot \|\hat{H}^\dagger\|) \delta \\ \mathcal{F}_2(\delta, \hat{\mathcal{Y}}) &:= (2\|\hat{K}_1\| + \mathcal{F}_1(\delta, \hat{\mathcal{Y}})) \mathcal{F}_1(\delta, \hat{\mathcal{Y}}) \\ \mathcal{F}_3(\delta, \hat{\mathcal{Y}}) &:= \sqrt{l_p} \left\| \hat{K}_2^\top \hat{K}_1 \right\| \delta + \left(\|\hat{b}(0)\| + \sqrt{l_p} \delta \right) \mathcal{F}_2(\delta, \hat{\mathcal{Y}}) \\ \mathcal{F}(\delta, \hat{\mathcal{Y}}) &:= \left\| (\hat{K}_2^\top \hat{K}_2 + I)^{-1} \right\| \mathcal{F}_3(\delta, \hat{\mathcal{Y}}) + \left(\left\| \hat{K}_2^\top \hat{K}_1 \hat{b}(0) \right\| + \mathcal{F}_3(\delta, \hat{\mathcal{Y}}) \right) \mathcal{F}_2(\delta, \hat{\mathcal{Y}}), \end{aligned} \tag{17}$$

where $\hat{K}_1 := \hat{Y}_f \hat{H}^\dagger$, $\hat{K}_2 := \hat{K}_1 [0 \ 0 \ I]^\top$ and $\hat{b}(u_f)$ is defined in (5). Then, by letting $\eta(\delta, \hat{\mathcal{Y}}) = 1 + \frac{\|\hat{H}^\dagger\| \mathcal{F}(\delta, \hat{\mathcal{Y}})}{\|\hat{g}(\hat{u}_f^*)\|}$, we have $\|\hat{u}_f^* - u_f^*\| \leq \mathcal{F}(\delta, \hat{\mathcal{Y}})$ and

$$\|\hat{g}(u_f^*)\| \leq \eta(\delta, \hat{\mathcal{Y}}) \|\hat{g}(\hat{u}_f^*)\|. \tag{18}$$

Recall that $c_{\text{worst}}(u_f)$ and $\bar{c}(u_f)$ are, respectively, the worst-case cost derived by the inner problem of (15) and the resulting true regulation cost when u_f is applied, u_f^* is the optimal input for the noiseless case (see (16)) and \tilde{u} is the optimal solution to (15). In the following, we compare $\bar{c}(\tilde{u}_f)$ with $\bar{c}(u_f^*)$ to see how much suboptimality is introduced by solving (15) and applying \tilde{u}_f .

Theorem 16. *Let Assumption 3, 5 and 8 hold and define*

$$\begin{aligned}\mathcal{C}_1(\delta, \hat{\mathcal{Y}}) &:= 2\sigma_{\min}^{-1}(\hat{H})(\sqrt{l_p} + \eta(\delta, \hat{\mathcal{Y}})l_h\|\hat{g}(\hat{u}_f^*)\|)\delta \\ \mathcal{C}_2(\delta, \hat{\mathcal{Y}}) &:= (\|\hat{Y}_f\| + l_h\delta)\mathcal{C}_1(\delta, \hat{\mathcal{Y}}) + \eta(\delta, \hat{\mathcal{Y}})l_h\|\hat{g}(\hat{u}_f^*)\|\delta \\ \mathcal{C}_3(\delta, \hat{\mathcal{Y}}) &:= 8(\mathcal{C}_2(\delta, \hat{\mathcal{Y}}))^2 + 4\|\hat{Y}_f\| \cdot \|\hat{g}(\hat{u}_f^*)\|\eta(\delta, \hat{\mathcal{Y}})\mathcal{C}_2(\delta, \hat{\mathcal{Y}}).\end{aligned}\tag{19}$$

One has that $\bar{c}(\tilde{u}_f) - \bar{c}(u_f^*) \leq \mathcal{C}_3(\delta, \hat{\mathcal{Y}})$. Moreover, the upperbound $\mathcal{C}_3(\delta, \hat{\mathcal{Y}})$, computable by using only the noisy measurements, converges in probability to 0 as δ converges to 0.

Proof. We denote $(\tilde{\Delta}_{Y_p}, \tilde{\Delta}_{Y_f}, \tilde{\Delta}_{y_p}, \tilde{g}(u_f))$ as the solution to the following optimization problem

$$\begin{aligned}\max_{\Delta_{Y_p}, \Delta_{Y_f}, \Delta_{y_p}, g} & g^\top (\hat{Y}_f + \Delta_{Y_f})^\top (\hat{Y}_f + \Delta_{Y_f})g + u_f^\top u_f \\ \text{s.t.} & \begin{bmatrix} U_p \\ \hat{Y}_p \\ U_f \end{bmatrix} g + \begin{bmatrix} 0 \\ \Delta_{Y_p} \\ 0 \end{bmatrix} g = \begin{bmatrix} u_p \\ \hat{y}_p \\ u_f^* \end{bmatrix} + \begin{bmatrix} 0 \\ \Delta_{y_p} \\ 0 \end{bmatrix} \\ & \max(\|\Delta_{Y_p}\|_{\max}, \|\Delta_{Y_f}\|_{\max}, \|\Delta_{y_p}\|_{\infty}) \leq \delta \\ & \|g - \hat{g}(u_f)\|^2 \leq \mathcal{C}^2(u_f)\delta^2\end{aligned}\tag{20}$$

and also define $\tilde{y}_f(u_f) := (\hat{Y}_f + \tilde{\Delta}_{y_f})\tilde{g}(u_f)$. Since $\|\hat{g}(u_f^*) - \bar{g}(u_f^*)\| \leq \mathcal{C}(u_f^*)\delta$ according to Theorem 10, we have

$$\begin{aligned}\frac{1}{2}\sigma_{\min}(\hat{H})\|\hat{g}(u_f^*) - \bar{g}(u_f^*)\| &\leq (\sqrt{l_p} + l_h\|\hat{g}(u_f^*)\|)\delta \\ &\leq (\sqrt{l_p} + \eta(\delta, \hat{\mathcal{Y}})l_h\|\hat{g}(\hat{u}_f^*)\|)\delta,\end{aligned}\tag{21}$$

where $\eta(\delta, \hat{\mathcal{Y}})$ is derived in Lemma 15. The inequality (21) implies $\|\hat{g}(u_f^*) - \bar{g}(u_f^*)\| \leq \mathcal{C}_1(\delta, \hat{\mathcal{Y}})$. Similarly, we have $\|\hat{g}(u_f^*) - \tilde{g}(u_f^*)\| \leq \mathcal{C}_1(\delta, \hat{\mathcal{Y}})$. Consequently, we can derive

$$\begin{aligned}\|\hat{y}_f(u_f^*) - \bar{y}_f(u_f^*)\| &= \|\hat{Y}_f(\hat{g}(u_f^*) - \bar{g}(u_f^*)) - \bar{\Delta}_{Y_f}\bar{g}(u_f^*)\| \\ &\leq \|\hat{Y}_f\| \cdot \|\hat{g}(u_f^*) - \bar{g}(u_f^*)\| + \|\bar{\Delta}_{Y_f}\| \cdot \|\bar{g}(u_f^*)\| \\ &\leq \|\hat{Y}_f\| \cdot \|\hat{g}(u_f^*) - \bar{g}(u_f^*)\| + \\ &\quad l_h\delta(\|\hat{g}(u_f^*)\| + \|\bar{g}(u_f^*) - \hat{g}(u_f^*)\|) \\ &\leq \underbrace{(\|\hat{Y}_f\| + l_h\delta)\mathcal{C}_1(\delta, \hat{\mathcal{Y}}) + \eta(\delta, \hat{\mathcal{Y}})l_h\|\hat{g}(\hat{u}_f^*)\|}_{\mathcal{C}_2(\delta, \hat{\mathcal{Y}})}\delta,\end{aligned}\tag{22}$$

$\|\hat{y}(u_f^*) - \tilde{y}(u_f^*)\| \leq \mathcal{C}_2(\delta, \hat{\mathcal{Y}})$ and $\|\bar{y}(u_f^*) - \tilde{y}(u_f^*)\| \leq 2\mathcal{C}_2(\delta, \hat{\mathcal{Y}})$. Finally, since \tilde{u}_f is the solution to the outer problem of (15) while u_f^* is feasible, $c_{\text{worst}}(\tilde{u}_f) \leq c_{\text{worst}}(u_f^*) = \|\tilde{y}_f(u_f^*)\|^2 + \|u_f^*\|^2$, based on which we have

$$\begin{aligned}
\bar{c}(\tilde{u}_f) - \bar{c}(u_f^*) &\leq c_{\text{worst}}(\tilde{u}_f) - \bar{c}(u_f^*) \\
&\leq c_{\text{worst}}(u_f^*) - \bar{c}(u_f^*) \\
&= \|\tilde{y}_f(u_f^*)\|^2 + \|u_f^*\|^2 - \bar{c}(u_f^*) \\
&\leq \|\bar{y}_f(u_f^*)\|^2 + \|u_f^*\|^2 + \|\tilde{y}_f(u_f^*) - \bar{y}_f(u_f^*)\|^2 - \bar{c}(u_f^*) + \\
&\quad 2(\|\hat{y}_f(u_f^*)\| + \|\bar{y}_f(u_f^*) - \hat{y}_f(u_f^*)\|) \cdot \|\tilde{y}_f(u_f^*) - \bar{y}_f(u_f^*)\| \\
&\leq 2(\eta(\delta, \hat{\mathcal{Y}}) \|\hat{Y}_f\| + \|\hat{g}(\hat{u}_f^*)\| + \mathcal{C}_2(\delta, \hat{\mathcal{Y}})) \cdot 2\mathcal{C}_2(\delta, \hat{\mathcal{Y}}) + 4(\mathcal{C}_2(\delta, \hat{\mathcal{Y}}))^2 \\
&= \underbrace{8(\mathcal{C}_2(\delta, \hat{\mathcal{Y}}))^2 + 4 \|\hat{Y}_f\| \cdot \|\hat{g}(\hat{u}_f^*)\| \eta(\delta, \hat{\mathcal{Y}}) \mathcal{C}_2(\delta, \hat{\mathcal{Y}})}_{\mathcal{C}_3(\delta, \hat{\mathcal{Y}})}.
\end{aligned} \tag{23}$$

As δ goes to 0, the noisy measurement $\hat{\mathcal{Y}}$ converges in probability to $\bar{\mathcal{Y}} := (Y_p, Y_f, y_p)$. Therefore, we see that $\sigma_{\min}^{-1}(\hat{H})$ converges in probability to $\sigma_{\min}^{-1}(\bar{H})$, $\eta(\delta, \hat{\mathcal{Y}})$ to 1 and thus $\mathcal{C}_3(\delta, \hat{\mathcal{Y}})$ to 0. \square

Now, we see that as the measurement noise diminishes, the regulation cost resulting from the solution to (15) decreases to the minimal value. This is different from the suboptimality bound in [15] where the achieved regulation cost is only shown to be less than twice the minimal value.

Remark 17. If the measurement noise sequence is i.i.d., by sampling the same historical trajectories for N times to construct $\hat{Y}_{p,i}, \hat{Y}_{f,i}, \hat{y}_{p,i}$ for $i = 1, \dots, N$ (representing instances of Y_p, Y_f, y_p with independent noise realizations) and calculating the average values $\hat{Y}_p^{\text{avg}} = (1/N) \sum_{i=1}^N \hat{Y}_{p,i}$, $\hat{Y}_f^{\text{avg}} = (1/N) \sum_{i=1}^N \hat{Y}_{f,i}$, $\hat{y}_p^{\text{avg}} = (1/N) \sum_{i=1}^N \hat{y}_{p,i}$, we can attenuate the influence of noise. Specifically, given any $\epsilon > 0$, there exists $0 < \delta^{\text{new}}(N, \epsilon) < \delta$ such that $\delta^{\text{new}}(N, \epsilon)$ converges to 0 as N goes to infinity and

$$\max\{\|\hat{Y}_p^{\text{avg}} - Y_p\|_{\max}, \|\hat{Y}_f^{\text{avg}} - Y_f\|_{\max}, \|\hat{y}_p^{\text{avg}} - y_p\|_{\max}\} \leq \delta^{\text{new}}(N, \epsilon)$$

holds with a probability of $1 - \epsilon$. The averaging technique can be used to satisfy Assumption 8. Moreover, it allows one to conduct a sampling complexity analysis for the robust control scheme (15) (i.e., upperbounding the number of samples required to achieve a given suboptimality level), similar with the ones conducted in [6], [23] for model-based schemes.

Remark 18. If the formulation (15) is extended to solve a trajectory tracking problem with an objective function $\|y_f - y_{\text{ref}}\|_Q + \|u_f\|_R$ with positive semidefinite matrices $Q \in \mathbb{R}^{p \times p}$ and $R \in \mathbb{R}^{m \times m}$, it is easy to modify Theorem 16 for upperbounding the suboptimality gap.

V. EXTENSIONS

A. Extensions to MIMO systems

According to Remark 7, for MIMO systems we cannot bound the prediction error $\|\hat{y}(u_f) - \bar{y}(u_f)\|$ resulting from the scheme (5) and thus cannot analyse the suboptimality of our robust control framework (15). Here, we propose a method where Page matrices are built separately for each output.

Suppose we have outputs y^1, y^2, \dots, y^p . For each output y^i , we have a MISO sub-system with minimal realization

$$\begin{aligned} x_{t+1}^i &= A^i x_t^i + B^i u_t, \\ y_t^i &= C^i x_t^i + D^i u_t, \end{aligned} \quad (24)$$

where the matrices A^i, B^i, C^i, D^i are unknown. We build, according to (6), the Page matrices $U_p^i, U_f^i, \hat{Y}_p^i, \hat{Y}_f^i, \hat{H}^i$ along with the recent vectors $u_p^i, u_f^i, \hat{y}_p^i$ for each i . Similar with (15), we can write the robust control problem as

$$\min_{u_f} \max_{\Delta, g, y_f} \|u_f\|^2 + \sum_{i=1}^n \|y_f^i\|^2 \quad (25a)$$

$$\text{s.t. } \forall i, \begin{bmatrix} U_p^i \\ \hat{Y}_p^i \\ U_f^i \\ \hat{Y}_f^i \end{bmatrix} g^i + \begin{bmatrix} 0 \\ \Delta_{Y_p}^i \\ 0 \\ \Delta_{Y_f}^i \end{bmatrix} g^i = \begin{bmatrix} u_p^i \\ \hat{y}_p^i \\ u_f^i \\ y_f^i \end{bmatrix} + \begin{bmatrix} 0 \\ \Delta_{y_p}^i \\ 0 \\ 0 \end{bmatrix} \quad (25b)$$

$$\max \left(\|\Delta_{Y_p}^i\|_{\max}, \|\Delta_{Y_f}^i\|_{\max}, \|\Delta_{y_p}^i\|_{\infty} \right) \leq \delta \quad (25c)$$

$$\|g^i - \hat{g}^i(u_f)\|^2 \leq (C^i(u_f)\delta)^2, \quad (25d)$$

where $C^i(u_f) = 2\sigma_{\min}^{-1}(\hat{H}^i)(\sqrt{l_p^i} + l_h^i \|\hat{g}^i(u_f)\|)$.

To justify this formulation, we notice that, Theorem 14 and 16 can be applied to every sub-system in (24). Summing up all the suboptimality bounds, we can get the suboptimality bound for the whole system. The alternating method in [22] is also applicable to solve (25).

B. Extensions to account for input and output constraints

Suppose now there are an input constraint $u_f \in \mathcal{U}$ and an output constraint $(\bar{y}_f^1(u_f), \dots, \bar{y}_f^p(u_f)) \in \mathcal{Y}$. The input constraint $u_f \in \mathcal{U}$ can be easily embedded into the outer optimization problem in (15). To ensure satisfaction of the output constraint, we have to consider the prediction error and regard as infeasible the sequence u_f that has the slightest chance of violating the output constraint. By applying the inequalities in Theorem 10 to every MISO subsystem, we derive the prediction error bound $\mathcal{E}^i(u_f, \delta)$ for the i -th

output, i.e., $\|\hat{y}_f^i(u_f) - \bar{y}_f^i(u_f)\| \leq \mathcal{E}^i(u_f, \delta)$. Therefore, we can guarantee that $\bar{y}_f^i(u_f) \in \mathcal{B}(\hat{y}_f^i(u_f), \mathcal{E}^i(u_f, \delta))$.

Let

$$\mathcal{Y}_f(u_f) := \{(y_f^1, \dots, y_f^p) | y_f^i \in \mathcal{B}(\hat{y}_f^i(u_f), \mathcal{E}^i(u_f, \delta)), \forall i\}$$

be the region where the output sequence might lie. Then, we can ensure the satisfaction of the output constraints by enforcing the input in (25) to additionally verify that

$$\mathcal{Y}_f(u_f) \subset \mathcal{Y}. \quad (26)$$

We call the optimization problem (25) under (26) Safe Data-Driven Minmax Control (SDDMC). Enforcing (26) for general \mathcal{Y} can be challenging [24]. However, if

$$\mathcal{Y} = \{(\bar{y}_f^1, \dots, \bar{y}_f^p) | y_-^i \leq \bar{y}_f^i \leq y_+^i, \forall i\}$$

is a box constraint, the constraint (26) translates to another box constraint, which is for any i ,

$$y_-^i + \mathcal{E}^i(u_f, \delta) \leq \hat{y}_f^i(u_f) \leq y_+^i - \mathcal{E}^i(u_f, \delta). \quad (27)$$

VI. NUMERICAL STUDIES

In this section, through numerical experiments, we elaborate on the implementation details, verify the theoretical results and test the performance of SDDMC.

A. Trajectory regulation for a SISO system

To begin with, we consider a SISO system with the following system matrices

$$A = 0.99 * \begin{bmatrix} 0.7 & 0.2 & 0 \\ 0.3 & 0.7 & -0.1 \\ 0 & -0.2 & 0.8 \end{bmatrix}, B = \begin{bmatrix} 1 \\ 2 \\ 1.5 \end{bmatrix}, C = \begin{bmatrix} 1 & 1 & 1 \end{bmatrix}, D = 0. \quad (28)$$

We assume these matrices along with the observability index $l_o = 3$ are unknown to us. We aim to identify the observability index l_o , construct the relevant Page matrices, observe the trajectory prediction error and then solve a robust control problem.

We collect historical data by exciting the system according to (6) with $\mathcal{Q} = \mathcal{N}(0, 4)$, $L = 8$ and $T = 160$. The i.i.d. measurement noise in the simulation is sampled from the uniform distribution on $[-\delta, \delta]$ with $\delta = 10^{-3}$. Algorithm 1 returns the correct observability index $l_o = 3$. Now we can derive the matrices U_p, U_f, Y_p, Y_f according to Assumption 5. We use (5) to predict the future output with a horizon of length 3 following a fixed recent trajectory. We notice that if \hat{H} is constructed using (5) and (4) with $l_p = l_o = 3$, the prediction error is 1.8×10^{-2} . If we set $l_p = 4$, the error becomes 1.4×10^4 .

Through this comparison, we see the important role of observability index identification for the prediction scheme (5).

We then test our robust control scheme (15) on the SISO system (28). With $l_p = l_f = 3$ and the recent trajectory (u_p, y_p) where $u_p = [-5.2254, 7.2684, -22.5535]^\top$ and $y_p = [-1.1242, -23.7291, 13.3406]^\top$, we aim to achieve a minimum regulation cost $\bar{c}(u_f) = 10u_f^\top * u_f + \bar{y}_f(u_f)^\top \bar{y}_f(u_f)$. We use the scheme (15) to address this regulation problem.

We elaborate on how to solve (15). To use the alternating method, we initialize the input sequence by $u_f = \hat{u}_f^*$ (defined in (16)). When the input is fixed, the inner maximization problem of (15) is solved through IPOPT [25] using the primal-dual barrier approach, where the feasible solution $(\Delta_{Y_p}, \Delta_{Y_f}, \Delta_{y_p}, g) = (0, 0, \hat{Y}_p \hat{g}(u_f) - \hat{y}_p, \hat{g}(u_f))$ is set as the initial point. After deriving $(\tilde{\Delta}_{Y_p}, \tilde{\Delta}_{Y_f}, \tilde{\Delta}_{y_p}, \tilde{g})$, the solution to the inner problem, the outer problem of (15) is simply

$$\min_{u_f} \tilde{G}(\tilde{\Delta}_{Y_p}, \tilde{\Delta}_{Y_f}, \tilde{\Delta}_{y_p}, \tilde{g}, u_f) := \left\| \begin{pmatrix} \tilde{Y}_f + \tilde{\Delta}_{Y_f} \\ \tilde{Y}_p + \tilde{\Delta}_{Y_p} \\ U_f \end{pmatrix}^\dagger \begin{bmatrix} U_p \\ y_p + \tilde{\Delta}_{y_p} \\ u_f \end{bmatrix} \right\| + \|u_f\|^2,$$

where the objective is a quadratic function of u_f and the explicit expression of the solution can be readily computed. With the new input sequence at hand, we can start the next iteration. We terminate this algorithm when the difference of input sequences derived in two iterations has a 2-norm less than 10^{-4} . Currently, we do not have any results on the convergence for this iterative scheme. Empirically, we observe in solving the regulation problem defined above that at most three iterations are needed before the termination even when δ increases to 1.

Then, we solve 50 instances of the regulation problem with independent noise realizations. To evaluate the performance of the control scheme (15), we calculate for each instance the relative suboptimality, defined as $\frac{\bar{c}(\hat{u}_f) - \bar{c}(u_f^*)}{\bar{c}(\hat{u}_f)}$. In Fig. 1, we show the mean relative suboptimality for different δ . We see that the input sequence derived based on (15) and the alternating method achieves a suboptimality gap that decreases to 0 as the noise diminishes, which coincides with Theorem 16. Although we find that with $\delta > 10^{-2}$ Assumption 8 is not satisfied and thus Theorem 16 is not valid, the relative suboptimality resulting from the robust control scheme (26) is empirically small even when $\delta = 1$. When the measurement noise is i.i.d., we can weaken Assumption 8 such that Theorem 6 and Theorem 16 are valid for larger noise level for a high probability. However, to achieve this, we need to use random matrix analysis to tighten (11), which is out of the scope of this paper.

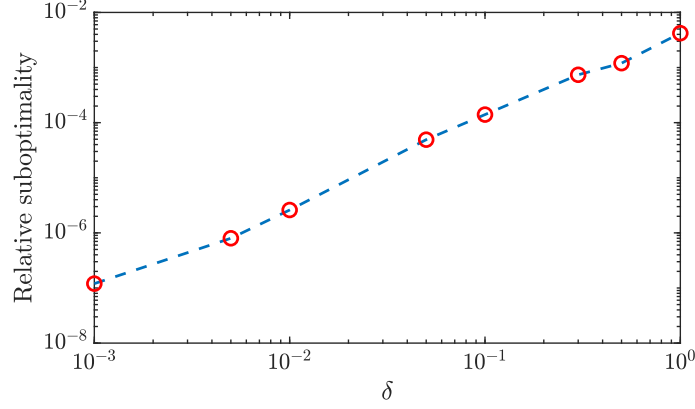


Fig. 1. Mean relative suboptimality for different δ

B. Application to a MIMO system with constraints: room temperature control

We apply Safe Data-Driven Minmax Control (SDDMC) proposed in Section V-B to room temperature control. We consider a small building model taken from [26], where the temperature dynamic is normalized and linearized at the equilibrium temperature $T = 15^\circ\text{C}$ (which coincides with the outdoor temperature), with a sampling time of 0.5 hour. The model is described by (*), with

$$A = \begin{bmatrix} 0.8511 & 0.0541 & 0.0707 \\ 0.1293 & 0.8635 & 0.0055 \\ 0.0989 & 0.0032 & 0.7541 \end{bmatrix}, \quad B = \begin{bmatrix} 0.07 \\ 0.006 \\ 0.004 \end{bmatrix}, \quad C = \begin{bmatrix} 1 & 0 & 0 \\ 0 & 1 & 0 \end{bmatrix}, \quad D = 0.$$

The three states represent the temperature at different spots while only two of them can be measured as indicated in the matrix C . Notice that, due to normalization, a state with a value x translates to $(x+15)^\circ\text{C}$ at the corresponding spot. We assume that, at time $t = 0$, the system is at equilibrium. Therefore, the indoor and outdoor temperature is 15°C . To increase the indoor temperature to 25°C and balance between user comfort and energy consumption, we let the cost function be $\bar{c}(u_f) = 10u_f^\top * u_f + (\bar{y}_f(u_f) - 10 * [1 \ 1]^\top)^\top (\bar{y}_f(u_f) - 10 * [1 \ 1]^\top)$ covering the horizon $0 \leq t \leq 4$, while enforcing the the first output to be no less than 5 for $t \geq 1$, i.e., the first spot to be at least 20°C in half an hour after the experiment starts.

We run SDDMC in 50 experiments with independent noise realizations ($\delta = 0.01$). We show in Fig. 2 the trajectory of the first output. We also compare with PEM in [20] where the prediction given by (5) is regarded as the true output. From Fig. 2, we observe that the lower bound 20°C for the first output is always satisfied if SDDMC is applied while PEM generates several trajectories with constraint violations. Meanwhile, we also plot the mean relative suboptimality in Fig. 3 for different δ . The suboptimality decreases to 0 when δ diminishes. A source of suboptimality, when δ gets larger, is the conservative

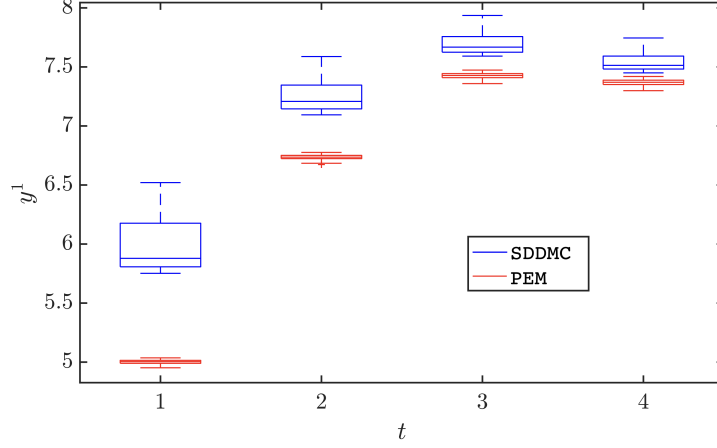


Fig. 2. Trajectory of the first output: SDDMC v.s. PEM ($\delta = 0.01$)

estimate of the prediction error bound. This is also the main reason why in Fig. 2 the output trajectory is substantially far away from the constraint boundaries. If one can shrink the uncertainty set, the output trajectory can get closer to the boundary, therefore leading to better optimality.

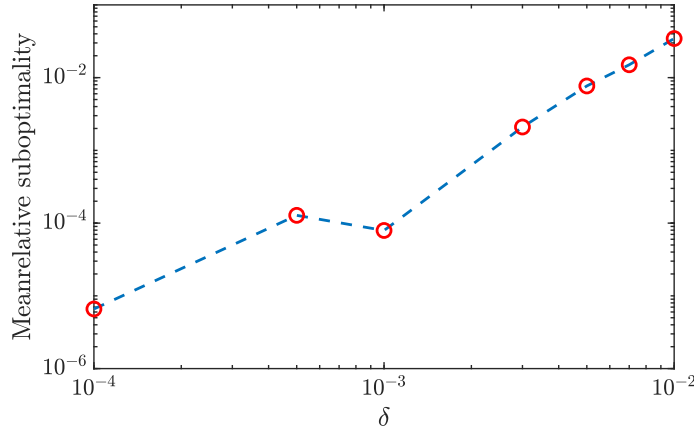


Fig. 3. Room temperature control: mean relative suboptimality for different δ

VII. CONCLUSION

In this paper, we proposed a method to construct the Page matrices for linear system trajectory prediction such that the error due to the measurement noise can be bounded using solely collected data. Based on this error bound, we designed the minimax robust control scheme such that the suboptimality gap is bounded. This scheme is extended to solve regulation problems for MIMO systems with input/output

constraints. The experiments illustrated that with our method of Page matrix construction, we can achieve small prediction error and, by using the proposed robust control method, the suboptimality gap can be small for unconstrained optimal control problems. For constrained problems, we saw that the constraints were respected for different noise realizations. Our future studies will be focused on the design of historical input sequences for the derivation of a less conservative prediction error upperbound and on the development of robust control schemes with a reduced suboptimality gap.

REFERENCES

- [1] A. Tsiamis, I. Ziemann, N. Matni, and G. J. Pappas, “Statistical learning theory for control: A finite sample perspective,” *arXiv preprint arXiv:2209.05423*, 2022.
- [2] A. Karimi and C. Kammer, “A data-driven approach to robust control of multivariable systems by convex optimization,” *Automatica*, vol. 85, pp. 227–233, 2017.
- [3] M. Athans, “The role and use of the stochastic linear-quadratic-gaussian problem in control system design,” *IEEE transactions on automatic control*, vol. 16, no. 6, pp. 529–552, 1971.
- [4] H. K. Khalil, *Nonlinear control*, vol. 406. Pearson New York, 2015.
- [5] L. Ljung, *System Identification: Theory for the User*. Prentice Hall information and system sciences series, Prentice Hall PTR, 1999.
- [6] S. Dean, H. Mania, N. Matni, B. Recht, and S. Tu, “On the sample complexity of the linear quadratic regulator,” *Foundations of Computational Mathematics*, vol. 20, no. 4, pp. 633–679, 2020.
- [7] S. Oymak and N. Ozay, “Non-asymptotic identification of lti systems from a single trajectory,” in *2019 American control conference (ACC)*, pp. 5655–5661, IEEE, 2019.
- [8] M. Yin, A. Iannelli, and R. S. Smith, “Maximum likelihood estimation in data-driven modeling and control,” *IEEE Transactions on Automatic Control*, 2021.
- [9] Y. Lian, J. Shi, M. P. Koch, and C. N. Jones, “Adaptive robust data-driven building control via bi-level reformulation: an experimental result,” *arXiv preprint arXiv:2106.05740*, 2021.
- [10] J. Coulson, J. Lygeros, and F. Dörfler, “Data-enabled predictive control: In the shallows of the deepc,” in *2019 18th European Control Conference (ECC)*, pp. 307–312, IEEE, 2019.
- [11] J. C. Willems, P. Rapisarda, I. Markovsky, and B. L. De Moor, “A note on persistency of excitation,” *Systems & Control Letters*, vol. 54, no. 4, pp. 325–329, 2005.
- [12] L. Furieri, B. Guo, A. Martin, and G. Ferrari-Trecate, “Near-optimal design of safe output feedback controllers from noisy data,” *IEEE Transactions on Automatic Control*, 2022.
- [13] L. Kilian, “Finite-sample properties of percentile and percentile-t bootstrap confidence intervals for impulse responses,” *Review of Economics and Statistics*, vol. 81, no. 4, pp. 652–660, 1999.
- [14] L. Xu, M. S. Turan, B. Guo, and G. Ferrari-Trecate, “A data-driven convex programming approach to worst-case robust tracking controller design,” *arXiv preprint arXiv:2102.11918*, 2021.
- [15] L. Huang, J. Zhen, J. Lygeros, and F. Dörfler, “Robust data-enabled predictive control: Tractable formulations and performance guarantees,” *arXiv preprint arXiv:2105.07199*, 2021.
- [16] J. Berberich, J. Köhler, M. A. Müller, and F. Allgöwer, “Data-driven model predictive control with stability and robustness guarantees,” *IEEE Transactions on Automatic Control*, vol. 66, no. 4, pp. 1702–1717, 2020.

- [17] J. Coulson, H. van Waarde, and F. Dörfler, “Robust fundamental lemma for data-driven control,” *International Symposium on Mathematical Theory of Networks and Systems*, 2022.
- [18] J. Coulson, H. J. Van Waarde, J. Lygeros, and F. Dörfler, “A quantitative notion of persistency of excitation and the robust fundamental lemma,” *IEEE Control Systems Letters*, vol. 7, pp. 1243–1248, 2022.
- [19] J. Coulson, J. Lygeros, and F. Dörfler, “Distributionally robust chance constrained data-enabled predictive control,” *arXiv preprint arXiv:2006.01702*, 2020.
- [20] L. Huang, J. Coulson, J. Lygeros, and F. Dörfler, “Data-enabled predictive control for grid-connected power converters,” in *2019 IEEE 58th Conference on Decision and Control (CDC)*, pp. 8130–8135, IEEE, 2019.
- [21] R.-C. Li, “Relative perturbation theory: I. eigenvalue and singular value variations,” *SIAM Journal on Matrix Analysis and Applications*, vol. 19, no. 4, pp. 956–982, 1998.
- [22] S. Lu, I. Tsaknakis, and M. Hong, “Block alternating optimization for non-convex min-max problems: algorithms and applications in signal processing and communications,” in *ICASSP 2019-2019 IEEE International Conference on Acoustics, Speech and Signal Processing (ICASSP)*, pp. 4754–4758, IEEE, 2019.
- [23] L. Xu, B. Guo, and G. Ferrari-Trecate, “Finite-sample-based spectral radius estimation and stabilizability test for networked control systems,” *arXiv e-prints*, pp. arXiv–2103, 2021.
- [24] J. Guthrie, M. Kobilarov, and E. Mallada, “Closed-form minkowski sum approximations for efficient optimization-based collision avoidance,” in *2022 American Control Conference (ACC)*, pp. 3857–3864, IEEE, 2022.
- [25] A. Wächter and L. T. Biegler, “On the implementation of an interior-point filter line-search algorithm for large-scale nonlinear programming,” *Mathematical programming*, vol. 106, no. 1, pp. 25–57, 2006.
- [26] F. Oldewurtel, C. N. Jones, and M. Morari, “A tractable approximation of chance constrained stochastic mpc based on affine disturbance feedback,” in *2008 47th IEEE conference on decision and control*, pp. 4731–4736, IEEE, 2008.
- [27] G. W. Stewart, “On the perturbation of pseudo-inverses, projections and linear least squares problems,” *SIAM review*, vol. 19, no. 4, pp. 634–662, 1977.

APPENDIX

A. A preliminary lemma for the proof of Theorem 6

Lemma 19. *If the system (*) is SISO and Assumption 5 holds, we let*

$$\mathcal{W} := \begin{bmatrix} u_{L+1} & \cdots & u_{2L} \\ u_{3L+1} & \cdots & u_{4L} \\ \vdots & \vdots & \vdots \\ u_{2Ll_L-L+1} & \cdots & u_{2Ll_L} \end{bmatrix}, \quad \mathcal{X} := \begin{bmatrix} Cx_{L+1} & \cdots & CA^{l_p-1}x_{L+1} \\ Cx_{3L+1} & \cdots & CA^{l_p-1}x_{3L+1} \\ \vdots & \vdots & \vdots \\ Cx_{2Ll_L-L+1} & \cdots & CA^{l_p-1}x_{2Ll_L-L+1} \end{bmatrix},$$

$$\text{and } \mathcal{V} := \begin{bmatrix} \mathcal{W} & \mathcal{X} \end{bmatrix}. \quad (29)$$

Then

$$\mathbb{P}(\{\mathcal{V} \text{ is full rank}\}) = 1.$$

Proof. We first notice that $l_p = l_o \geq n_x$, otherwise, for a single-output system, $\mathcal{O}(l_p)$ cannot be column full rank. By the Cayley-Hamilton theorem, we know $\mathcal{O}(l_p)$ has the same row rank as $\mathcal{O}(n_x)$. Since

$\mathcal{O}(l_p)$ is full column rank, $\mathcal{O}(n_x)$ is also. According to Definition 4, $l = l_p$ is the smallest such that $\mathcal{O}(n_x)$ is full row rank and thus $l_p \leq n_x$. Considering these facts, we conclude that $l_p = n_x$. Now we proceed by proving that the event $F_{\mathcal{X}} = \{\mathcal{X}_{1:l_p, \cdot} \text{ is full row rank}\}$ takes place almost surely.

In order to show $\mathbb{P}(F_{\mathcal{X}}) = 1$, we use an induction argument. We first look into the first row of \mathcal{X} . According to the system dynamic (*), we have

$$x_{L+1} = \begin{bmatrix} B & AB & \cdots & A^{L-1}B \end{bmatrix} \begin{bmatrix} u_L & u_{L-1} & \cdots & u_1 \end{bmatrix}^\top, \quad \mathcal{X}_{1, \cdot} = x_{L+1}^\top \mathcal{O}(l_p)^\top. \quad (30)$$

Since $x_{L+1} = 0$ defines a subspace in \mathbb{R}^{mL} where $u_{[1,L]}$ resides, by using (7) we have $\mathbb{P}\{\mathcal{X}_{1, \cdot} = 0\} = \mathbb{P}\{x_{L+1} = 0\} = 0$. Then, in the following, we show that, for any $l < l_p$,

$$\mathbb{P}\{\mathcal{X}_{1:(l+1), \cdot} \text{ has row full rank} | \mathcal{X}_{1:l, \cdot} \text{ has row full rank}\} = 1. \quad (31)$$

To this end, we let Θ be the event where the inputs are fixed from $t = 1$ to $t = (2l-1)L$ and suppose $\Theta \in \{\mathcal{X}_{1:l, \cdot} \text{ has row full rank}\}$, then there exists a vector $x_n \in \mathbb{R}^{l_p}$ and $x_n \neq 0$ such that $\mathcal{X}_{i, \cdot} x_n = 0$ holds for any $i \leq l$. If $\mathcal{X}_{1:(l+1), \cdot}$ does not have full rank, we have

$$\mathcal{X}_{l+1, \cdot} x_n = 0. \quad (32)$$

By noticing $\mathcal{X}_{l+1, \cdot} = x_{(2l+1)L+1}^\top \mathcal{O}(l_p)^\top$, we can rewrite (32) into

$$x_n^\top \mathcal{O}(l_p) x_{(2l+1)L+1} + x_n^\top \mathcal{O}(l_p) \begin{bmatrix} B & \cdots & A^{2L-1}B \end{bmatrix} \begin{bmatrix} u_{(2l+1)L} & \cdots & u_{(2l-1)L+1} \end{bmatrix}^\top = 0. \quad (33)$$

By noticing that $\mathcal{O}(l_p)$ is full rank and $x_n^\top \mathcal{O}(l_p) \neq 0$, we see $x_n^\top \mathcal{O}(l_p) \begin{bmatrix} B & \cdots & A^{2L-1}B \end{bmatrix} \neq 0$ since $\begin{bmatrix} B & \cdots & A^{2L-1}B \end{bmatrix}$ is full row rank. Then, the realizations of $u_{(2l-1)L+1}, \dots, u_{(2l+1)L}$ avoids (33) almost surely due to (7). Therefore, the claim (31) holds because

$$\mathbb{P}\{\mathcal{X}_{1:(l+1), \cdot} \text{ has row full rank} | \Theta\} = 1.$$

Due to (31), if $l < l_p$ and $\mathbb{P}\{\mathcal{X}_{1:l, \cdot} \text{ has row full rank}\} = 1$, then $\mathbb{P}\{\mathcal{X}_{1:(l+1), \cdot} \text{ has row full rank}\} = 1$. By induction, we know $\mathbb{P}\{\mathcal{X}_{1:l_p, \cdot} \text{ has row full rank}\} = 1$.

Now, almost surely, the first l_p rows of \mathcal{X} are linear independent while the last L rows of \mathcal{W} are linear independent. Since the inputs in the (l_p+i) -th row of \mathcal{W} are independent of the elements in the (l_p+i) -th row of \mathcal{X} for $1 \leq i \leq L$, we can again use the induction technique to show that the first (l_p+i) rows of \mathcal{V} are linearly independent almost surely for $1 \leq i \leq L$. Thus, we have that $\mathbb{P}(\{\mathcal{V} \text{ is full rank}\}) = 1$. \square

B. Proof of Theorem 6

In this proof, we **only** considers single-input cases for simplicity since it can be easily adapted to multiple-input cases. The main idea is to exploit the relationship between \overline{H} and \mathcal{V} in Lemma 19.

We let $l_L = L + l_p$ and denote \overline{H}° as the submatrix consisting of the $2, 4, \dots, 2l_L$ -th columns of \overline{H} . We notice that for any i, j ,

$$y_{L(2i-1)+j} = CA^{j-1}x_{L(2i-1)+1} + \sum_{k=1}^{j-1} CA^k Bu_{L(2i-1)+k}. \quad (34)$$

By substituting (34) into \overline{H}° and using elementary row transformation to simplify \overline{H}° , we see that \overline{H}° is full row rank if \mathcal{V} , defined in (29), has full rank. From Lemma 19, we have that $\mathbb{P}(\{\overline{H} \text{ is full row rank}\}) \geq \mathbb{P}(\{\overline{H}^\circ \text{ is full row rank}\}) \geq \mathbb{P}(\{\mathcal{V} \text{ is full rank}\}) = 1$.

C. Proof of Proposition 11

The proof for the case $l_p < l_o$ is an easy modification of that for Theorem 6 and thus omitted. If $l_p > l_o$, we notice that there exist matrices $\mathcal{A}_i \in \mathbb{R}^{p \times p}$, $\mathcal{F}_i \in \mathbb{R}^{p \times m}$ for $1 \leq i \leq l_o$ such that the l_o th-order ARX model

$$y_t = \sum_{i=1}^{l_o} (\mathcal{A}_i y_{t-i} + \mathcal{F}_i u_{t-i}) \quad (35)$$

describes exactly the system (*). Therefore, we almost surely have that the $(l_o p + 1)$ -th row of Y_p is a linear combination of the first $l_o p$ rows of U_p and the first $l_o p$ rows of Y_p , which concludes the proof.

D. A supporting lemma for Proposition 12

Lemma 20. *Given a full-row-rank matrix $A \in \mathbb{R}^{m \times n}$ with $m < n$ and a row vector $z \in \mathbb{R}^{m \times n}$, we have that*

$$\sigma_{\min}([A^\top z^\top]^\top) \leq \sigma_{\min}(A).$$

Proof. According to the definition of singular values, we have

$$\begin{aligned} \sigma_{\min}([A^\top z^\top]^\top) &= \min_{v \in \mathbb{R}^{m+1}, \|v\|=1} \|[A^\top z^\top]v\| \\ &\leq \min_{v \in \mathbb{R}^{m+1}, \|v\|=1, v_{m+1}=0} \|[A^\top z^\top]v\| \\ &\leq \min_{w \in \mathbb{R}^m, \|w\|=1} \|A^\top w\| = \sigma_{\min}(A) \end{aligned} \quad (36)$$

□

E. Proof of Lemma 15

By substituting (5) to (16), we have

$$\hat{u}_f^* = \underset{u_f}{\operatorname{argmin}} (\hat{K}_1 \hat{b}(0) + \hat{K}_2 u_f)^\top (\hat{K}_1 \hat{b}(0) + \hat{K}_2 u_f) + u_f^\top u_f. \quad (37)$$

The solution is $\hat{u}_f^* = -(\hat{K}_2^\top \hat{K}_2 + I)^{-1} \hat{K}_2^\top \hat{K}_1 \hat{b}(0)$. With \bar{K}_1, \bar{K}_2 being the noiseless counterparts of \hat{K}_1, \hat{K}_2 respectively, we have $u_f^* = -(\bar{K}_2^\top \bar{K}_2 + I)^{-1} \bar{K}_2^\top \bar{K}_1 \bar{b}(0)$. In the following, we aim to bound $\|\hat{u}_f^* - u_f^*\|$.

Firstly, we analyse the influence of noise on \hat{K}_1 and \hat{K}_2 . Due to Assumption 8,

$$\sigma_{\min}(\bar{H}) \geq \sigma_{\min}(\hat{H}) - \|E\| \geq \frac{1}{2} \sigma_{\min}(\hat{H}).$$

Thus, $\|\bar{H}^\dagger\| = \sigma_{\min}^{-1}(\bar{H}) \leq 2\sigma_{\min}^{-1}(\hat{H})$. Considering the following conclusion in perturbation analysis [27],

$$\|\bar{H}^\dagger - \hat{H}^\dagger\| \leq 2 \max\{\|\bar{H}^\dagger\|^2, \|\hat{H}^\dagger\|^2\} \|E\| \quad (38)$$

we have $\|\bar{H}^\dagger - \hat{H}^\dagger\| \leq 8l_h \|\hat{H}^\dagger\|^2 \delta$ and

$$\begin{aligned} \|\hat{K}_1 - \bar{K}_1\| &\leq \|\hat{Y}_p\| \cdot \|\hat{H}^\dagger - \bar{H}^\dagger\| + \|\hat{Y}_p - Y_p\| \cdot \|\bar{H}^\dagger\| \\ &\leq 8l_h \|\hat{Y}_p\| \cdot \|\hat{H}^\dagger\|^2 \delta + 2l_h \|\hat{H}^\dagger\| \delta \\ &= \underbrace{2l_h \|\hat{H}^\dagger\| (1 + 4\|\hat{Y}_p\| \cdot \|\hat{H}^\dagger\|)}_{\mathcal{F}_1(\delta, \hat{\mathcal{Y}})} \delta. \end{aligned} \quad (39)$$

Therefore, $\|\hat{K}_2 - \bar{K}_2\| \leq \mathcal{F}_1 \delta$. Similarly we have

$$\max_{i=1,2} \left\{ \|\hat{K}_2^\top \hat{K}_i - \bar{K}_2^\top \bar{K}_i\| \right\} \leq \underbrace{(2\|\hat{K}_1\| + \mathcal{F}_1(\delta, \hat{\mathcal{Y}})) \mathcal{F}_1(\delta, \hat{\mathcal{Y}})}_{\mathcal{F}_2(\delta, \hat{\mathcal{Y}})}.$$

Secondly, again following (38), we have

$$(\hat{K}_2^\top \hat{K}_2 + I)^{-1} - (\bar{K}_2^\top \bar{K}_2 + I)^{-1} \leq 2\|\hat{K}_2^\top \hat{K}_2 - \bar{K}_2^\top \bar{K}_2\|. \quad (40)$$

Through the same technique for deducing (39) based on the upperbound of $\|\bar{H}^\dagger - \hat{H}^\dagger\|$, we utilize (40) to conclude that

$$\begin{aligned} \left\| \hat{K}_2^\top \hat{K}_1 \hat{b}(0) - \bar{K}_2^\top \bar{K}_1 \bar{b}(0) \right\| &\leq \underbrace{\sqrt{l_p} \|\hat{K}_2^\top \hat{K}_1\| \delta + \left(\|\hat{b}(0)\| + \sqrt{l_p} \delta \right) \mathcal{F}_2(\delta, \hat{\mathcal{Y}})}_{\mathcal{F}_3(\delta, \hat{\mathcal{Y}})}, \\ \|\hat{u}_f^* - u_f^*\| &\leq \underbrace{\left\| (\hat{K}_2^\top \hat{K}_2 + I)^{-1} \right\| \mathcal{F}_3(\delta, \hat{\mathcal{Y}}) + \left(\left\| \hat{K}_2^\top \hat{K}_1 \hat{b}(0) \right\| + \mathcal{F}_3(\delta, \hat{\mathcal{Y}}) \right) \mathcal{F}_2(\delta, \hat{\mathcal{Y}})}_{\mathcal{F}(\delta, \hat{\mathcal{Y}})} \end{aligned}$$

and $\mathcal{F}(\delta, \hat{\mathcal{Y}})$ converges to 0 as δ goes to 0.

Finally, we have $\|\hat{g}(u_f^*) - \hat{g}(\hat{u}_f^*)\| \leq \|\hat{H}^\dagger\| \cdot \|\hat{u}_f^* - u_f^*\|$ and then

$$\|\hat{g}(u_f^*)\| \leq \|\hat{g}(\hat{u}_f^*)\| + \|\hat{H}^\dagger\| \mathcal{F}(\delta, \hat{\mathcal{Y}}) = \|\hat{g}(\hat{u}_f^*)\| \left(1 + \frac{\|\hat{H}^\dagger\| \mathcal{F}(\delta, \hat{\mathcal{Y}})}{\|\hat{g}(\hat{u}_f^*)\|} \right). \quad (41)$$